Tellus (2006), 58B, 366–375
Printed in Singapore. All rights reserved

TELLUS

A direct carbon budgeting approach to infer carbon sources and sinks. Design and synthetic application to complement the NACP observation network

By CYRIL CREVOISIER[1]*, MANUEL GLOOR[1], ERWAN GLOAGUEN[1], LARRY W. HOROWITZ[2], JORGE L. SARMIENTO[1], COLM SWEENEY[3] and PIETER P. TANS[3], [1]*Atmospheric and Oceanic Sciences, Princeton University, Sayre Hall, Forrestal Campus, Princeton, NJ 08544, USA;* [2]*Geophysical Fluid Dynamics Laboratory, Forrestal Campus, 201 Forrestal Road, Princeton, NJ 08540-6649, USA;* [3]*NOAA/ESRL Global Monitoring Division (formerly CMDL), 325 Broadway R/GMD1, Boulder, CO 80305-3328, USA*

(Manuscript received 13 January 2006; in final form 28 June 2006)

ABSTRACT

In order to exploit the upcoming regular measurements of vertical carbon dioxide (CO_2) profiles over North America implemented in the framework of the North American Carbon Program (NACP), we design a direct carbon budgeting approach to infer carbon sources and sinks over the continent using model simulations. Direct budgeting puts a control volume on top of North America, balances air mass in- and outflows into the volume and solves for the surface fluxes. The flows are derived from the observations through a geostatistical interpolation technique called Kriging combined with transport fields from weather analysis. The use of CO_2 vertical profiles simulated by the atmospheric transport model MOZART-2 at the planned 19 stations of the NACP network has given an estimation of the error of 0.39 GtC yr^{-1} within the model world. Reducing this error may be achieved through a better estimation of mass fluxes associated with convective processes affecting North America. Complementary stations in the north-west and the north-east are also needed to resolve the variability of CO_2 in these regions. For instance, the addition of a single station near 52°N; 110°W is shown to decrease the estimation error to 0.34 GtC yr^{-1}.

1. Introduction

Determining the magnitude and cause of continental-scale carbon sources and sinks is fundamental to improving our current understanding of the carbon cycle and to allowing more accurate prediction of its future evolution. A common approach to characterizing carbon surface fluxes consists in using in situ observations of atmospheric carbon dioxide (CO_2) concentrations in an inverse modelling scheme (e.g. Gurney et al., 2004). However, most of the CO_2 observations used in such studies are ground-based measurements, and those located on land within or nearby vegetation are samples of a complicated signal, influenced by photosynthesis and respiration, vertical mixing in the boundary layer, frontal mixing and transport.

To provide more information on CO_2 distribution in the atmosphere and better constrain the inversions, measurements of vertical CO_2 profiles by aircraft and continuous measurements of atmospheric CO_2 on tall towers will soon be available at approximately 30 locations across North America, in the framework of the North American Carbon Program (NACP; plan available at http://www.isse.ucar.edu/nacp/). The goal of this network is to improve the knowledge of carbon uptake in this region, which current estimate is of the order of 0.9 GtC yr^{-1}, with an uncertainty ranging from 0.4 to 0.8 GtC yr^{-1} (Jacobson et al., in press). So far, the locations of 19 North American stations have been chosen. Vertical profiles have a lower spatial variance than surface measurements and provide integrated measures of the atmospheric CO_2 column that give insight into net surface fluxes over large areas.

Moreover, the NACP high-density observation network motivates the design of new CO_2 surface flux estimation methods, relying on observations only, and thereby avoiding the need for both a priori information and inversion of atmospheric transport, which is inherently unstable, as atmospheric flow is diffusive, but generally required in the commonly used Bayesian approaches. Such an approach may also avoid some problems caused by covariation of fluxes and atmospheric transport, the so-called rectification effect (Denning et al., 1995).

*Corresponding author.
e-mail: ccrevois@princeton.edu
DOI: 10.1111/j.1600-0889.2006.00214.x

This paper presents a new direct carbon budgeting approach that may be used to infer carbon sources and sinks in North America from NACP observations, its application to a synthetic case and its use to suggest a few additional stations to reinforce the NACP network. Section 2 details the NACP observation network and the simulations of CO_2 that will be used for the study. The design of the method, which gives insight into the behavior of atmospheric CO_2 over the continent and of the locations required for the stations, is presented in Section 3. Section 4 presents an interpolation technique used to infer CO_2 variations over North America from NACP sites and its use to determine the regions where stations are required. Conclusions and suggestions for further improvement of the method are given in Section 5.

2. Data

2.1. The NACP observation network

As part of the NACP, vertical profiles of CO_2, CO, CH_4, H_2, N_2O and SF_6 are measured by aircraft at various locations, along the coasts, in the interior of the USA, including Alaska, and throughout the South of Canada. At the time this paper was written, 19 stations were in operation. Their locations are given in Table 1 and plotted in Fig. 1 as crosses. Measurements of CO_2 vertical profiles are performed once to twice a week, from the surface to an altitude of 8 km, between 10 a.m. and 3 p.m., local time. Typically, the observed vertical gradients in CO_2 rarely exceed 12 ppmv between the surface and 500 m. At a few sites, complementary observations of $^{13}CO_2$, $^{14}CO_2$ or $^{18}O_2$ are available. The network is reinforced by flux towers and tall towers. The existing tall towers are shown as triangles on Fig. 1. They allow following the passage of weather systems, which have a major influence on trace gas fluxes and concentrations. Additional measurements of CO_2 and other gas vertical profiles will be performed at various locations during intensive campaigns.

Table 1. List of the 19 stations of the NACP network

Code	Site location	Latitude	Longitude
BERMS	Berms	53° 47′ N	104° 37′ W
BGI	Bradgate, Iowa	42° 49′ N	94° 24′ W
BNE	Beaver Crossing, Nebraska	40° 47′ N	97° 10′ W
CAR	Briggsdale, Colorado	40° 22′ N	104° 17′ W
CMA	Cape May	38° 58′ N	74° 28′ W
DND	Dahlen, North Dakota	48° 08′ N	97° 59′ W
ESP	Estevan Point, British Columbia	49° 34′ N	126° 22′ W
FWI	Fairchild, Wisconsin	44° 39′ N	90° 57′ W
HFM	Harvard Forest, Massachusetts	42° 32′ N	72° 10′ W
HIL	Homer, Illinois	40° 04′ N	87° 54′ W
LEF	Park Falls, Wisconsin	45° 55′ N	90° 16′ W
NHA	Worcester, Massachuset	42° 57′ N	70° 37′ W
OIL	Oglesby, Illinois	41° 16′ N	88° 56′ W
PFA	Poker Flat, Alaska	65° 04′ N	147° 17′ W
RIA	Rowley, Iowa	42° 23′ N	91° 50′ W
SCA	Summerville, South Carolina	32° 46′ N	79° 32′ W
SGP	Southern Great Plains, Oklahoma	36° 37′ N	97° 30′ W
TGC	Sinton, Texas	27° 43′ N	96° 51′ W
THD	Trinidad Head, California	41° 02′ N	124° 09′ W

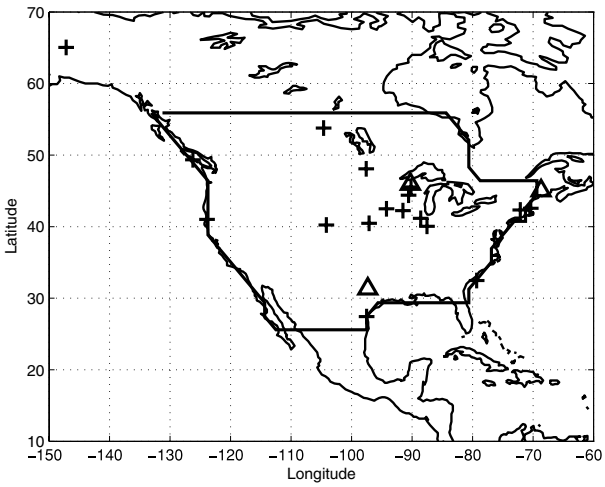

Fig. 1. Location of the 19 aircraft stations (crosses) and of the three tall tower sites (triangles) implemented as part of the NACP.

2.2. CO_2 simulations

To test the method and determine optimal additional station locations, use is made of CO_2 mixing ratio fields simulated by the atmospheric transport model MOZART-2 (Horowitz et al., 2003), driven by NCEP reanalysis with a $2^\circ \times 2^\circ$ spatial resolution and 29 levels in the vertical. Three surface flux components are used as surface boundary conditions: fossil fuel emissions, air-ocean fluxes and air-land fluxes.

Fossil fuel emissions are obtained in two steps. First, their spatial distribution is taken from emission estimates of fossil fuel burning, hydraulic cement production and gas flaring for 1995 obtained on a 1° gridcell basis by Andres et al. (1996). These patterns are then scaled on a monthly timescale using monthly fossil fuel emissions estimated by Blasing et al. (2004). It may be noted that, as they are based on population distribution, the patterns may not be accurate in developed countries such as the United States. Air-ocean fluxes are simulated by a new multiple element biogeochemical model of marine ecology developed at GFDL (J. P. Dunne, personal communication, 2005). Air-land fluxes are taken from net ecosystem production (NEP) simulations of the Carnegie–Ames–Stanford Approach (CASA) biosphere model (Randerson et al., 1997).

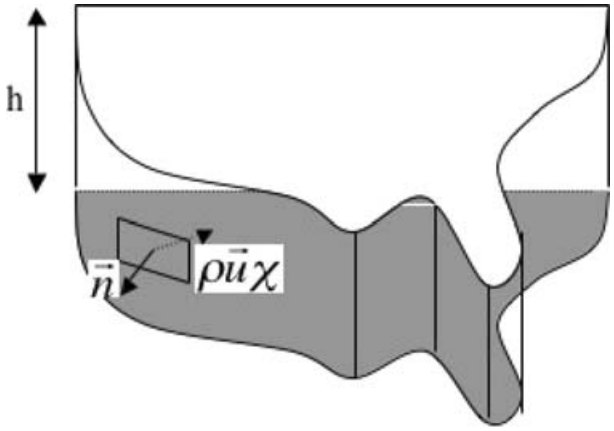

Fig. 2. Illustration of the carbon budgeting principle.

3. A direct carbon budgeting approach

3.1. Description of the method

Lets suppose we want to estimate surface fluxes in a given region (grey area in Fig. 2). The direct carbon budgeting approach consists in studying the variation of carbon within a control volume put over this region and extending from the surface to an altitude h. The carbon budget in this volume is given by the integrated continuity equation

$$\left.\frac{\partial C}{\partial t}\right|_V = \frac{\partial}{\partial t}\int\int\int_V \rho\chi \mathrm{d}V = -\int\int_S \rho\chi \boldsymbol{u}\boldsymbol{n}\mathrm{d}S + \left.\frac{\partial C}{\partial t}\right|_{\text{vertical}} + F_{\text{surf}}, \quad (1)$$

where V is the volume, C is the carbon mass content inside V, χ is the CO_2 mass mixing ratio, ρ is air density, $\boldsymbol{u}$ is the 3-D wind field, S is the surface enveloping V, $\boldsymbol{n}$ is the normal to S, t is time and F_{surf} is the carbon flux at the surface.

The first-term of eq. (1) represents the variation of carbon inside volume V during a time dt. The first-term of the right-hand side represents the fluxes of carbon due to advection and is the sum of the carbon fluxes going through the vertical edges and the top of the volume during dt. The second-term stands for the vertical carbon fluxes representing the exchanges, other than vertical advection, between the volume and the upper atmosphere, at an altitude h, during dt (mainly, the convection). The last-term, F_{surf}, represents the exchanges of carbon between the volume and the ground during dt; it stands for the surface fluxes we want to estimate.

To give insight on the expected variation of each term of eq. (1), we first assume that CO_2 vertical profiles are known at every grid point, using the CO_2 simulations presented in Section 2. Each term of eq. (1) can thus be computed: χ is given by the simulated profiles, $\boldsymbol{u}$ by the NCEP wind fields and the vertical carbon fluxes are simulated by MOZART-2. The surface fluxes are thus given by the following equation, which is a rewriting of eq. (1)

$$F_{\text{surf}} = \int\int_S \rho\chi \boldsymbol{u}\boldsymbol{n}\mathrm{d}S - \left.\frac{\partial C}{\partial t}\right|_{\text{vertical}} + \frac{\partial}{\partial t}\int\int\int_V \rho\chi \mathrm{d}V. \quad (2)$$

Following the planned vertical profile observation network, we have chosen a volume V over North America extending from 17°N to 54°N and from the western to the eastern coasts. The limits are plotted on Fig. 1. Volume V is chosen to vertically extend from the surface to an altitude of $h = 8$ km, which is the maximal altitude reached by the flights. As already mentioned, such an altitude may allow reducing the influence of the rectification effect, which stands for the covariance between terrestrial photosynthesis, boundary layer structure and cumulus convection that may result in a non-zero vertical gradient of several parts per million (ppm) in the annual mean CO_2 concentration over land for a zero net annual CO_2 flux (Denning et al., 1995). By avoiding the need for an explicit representation of boundary layer dynamics, the direct budgeting approach may reduce the influence of rectification on flux estimates. However, an altitude of 8 km may not be enough to cancel this effect when strong ventilation and deeper mixing of CO_2-depleted air occur during the day and the growing season. Our analysis will quantify magnitude reduction of the rectification signal with aircraft profile height and according recommendations on aircraft sampling.

The monthly variations of each term of eq. (2) derived from the simulations are plotted in Fig. 3. The vertical profiles of CO_2 being known for each gridcell inside volume V, the estimated surface fluxes F_{surf} (full line with dots), that are computed from the variation of carbon inside V (full line), the advective (dashed line) and convective (dashed line with dots) fluxes, are identical to the surface fluxes used for the simulations, as they must. The spatial variability and characteristics of each term are detailed in the following subsections.

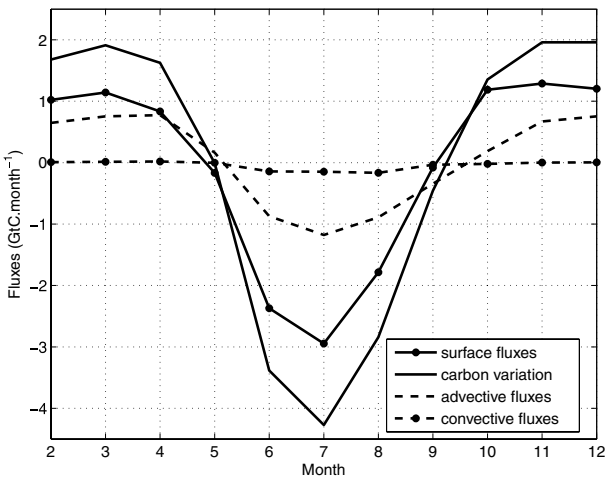

Fig. 3. Monthly evolution of each term of eq. (1): surface fluxes (full line with dots), carbon mass variation in volume V (full line), advective fluxes (dashed lines) and convective fluxes (dashed line with dots).

3.2. Surface fluxes

The surface fluxes over land are the sum of air-land fluxes and fossil fuel emissions. Figs. 4a and b show the standard variation of both CO_2 surface fluxes over 1 yr, which indicates where the highest variability of the fluxes are expected. The highest variations of air-land fluxes are found along a band extending from north-west to south-east and along the East coast, regions where most North American forests are found. Fossil fuel emissions come mainly from Texas, the East coast and, to a lesser extent, California. The highest CO_2 variations are expected where the surface fluxes are highly variable. More stations will thus be required in the North and along the East coasts to catch this variability. It can be seen on Fig. 1 that many stations are already located in most of these regions.

3.3. Advection

The advective fluxes are the sum of horizontal and vertical advective fluxes, as given by the following equation

$$\int\int_S \rho\chi\boldsymbol{u}\mathrm{d}S = \int\int_{S_{\mathrm{vert}}} \rho\chi(\boldsymbol{u}_x + \boldsymbol{u}_y)\mathrm{d}S_{\mathrm{vert}} + \int\int_{S_{\mathrm{top}}} \rho\chi\boldsymbol{u}_z\mathrm{d}S_{\mathrm{top}}, \quad (3)$$

where the notations follow those of eq. (1) and $\boldsymbol{u}_x$, $\boldsymbol{u}_y$ and $\boldsymbol{u}_z$ are the horizontal and vertical components of the wind field, S_{vert} is the surface of the vertical edges of volume V and S_{top} is the surface at the top of volume V. In the following, we examine the variations of horizontal fluxes that are the main component of advective fluxes.

At each gridcell along the horizontal edges of volume V, we use the CO_2 vertical profiles simulated by MOZART-2 along with the corresponding NCEP wind vertical profiles to compute the horizontal advection fluxes according to the first-term of the right-hand side of eq. (3). The annual average of their evolution along the edges is plotted on Fig. 5. A flux is positive when CO_2 enters the volume and negative when it leaves it. Summing the fluxes all along the edges of the volume gives the monthly evolution of the horizontal fluxes shown as dashed line on Fig. 3.

The flux evolution along the edges (see Fig. 5) indicates the incoming and outcoming pathways of CO_2 inside and outside volume V. CO_2 enters the volume from the West and the north-east; it leaves it in the East and, to a lesser extent, in the north-west. Influx and outflux through the southern edge of the volume nearly cancel each other. This evolution follows the wind distribution in North America, as can be seen on Fig. 5 which also shows the annual average NCEP wind field at an altitude of 4 km. Following the wind distribution, to well capture the evolution of CO_2 due to wind transport, more stations will thus be needed along the East and West coasts and on the northern part of the volume.

3.4. Convection

Figure 4c shows the annual standard deviation of CO_2 fluxes due to convection, at an altitude of 8 km (top of the volume), as computed by MOZART-2 driven by NCEP transport fields. Most of the variability comes from summer months. Indeed, over North America, high-reaching convection is mainly active in summer, from June to August, essentially in the South of

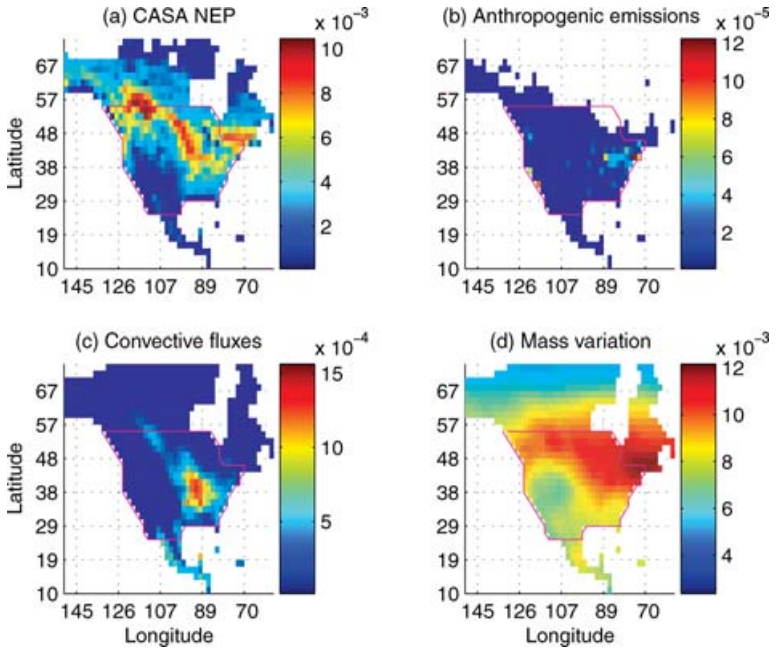

Fig. 4. Annual variability (standard deviation) of: (a) biospheric fluxes from CASA NEP; (b) anthropogenic emissions; (c) convective fluxes at an altitude of 8 km as computed by MOZART-2 and (d) carbon mass variation inside volume V. Units are GtC month^{-1}. Limits of volume V are shown as purple line.

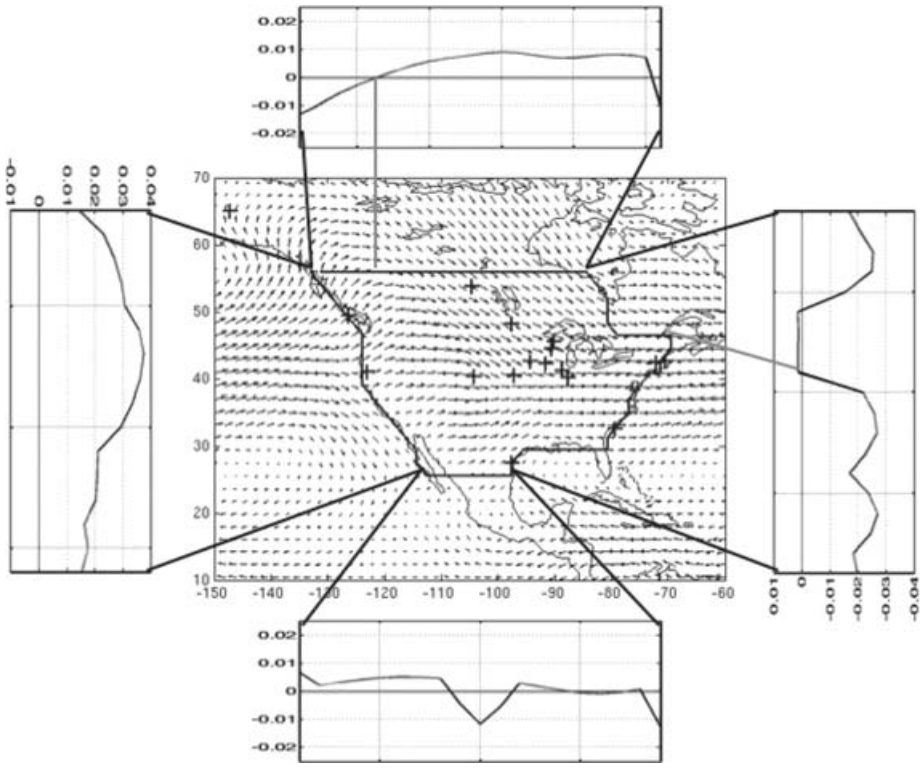

Fig. 5. Annual average of the evolution of advective fluxes along the edges of volume V (GtC month^{-1}). The central figure shows the annual mean of NCEP wind distribution at an altitude of 4 km. NACP stations are shown as crosses.

the USA. This phenomenon is known as the North American Monsoon (e.g. Adams and Comrie, 1997): the winds, which generally have a westerly component in winter and spring, tend to come more from the South (Caribbean Sea and Mexico) during summer and thus lead to convective instabilities associated with surface heating of moist oceanic air. Although this phenomenon affects the whole southern USA, the CO_2 convection fluxes are mainly found in the south-east, following the high-variability of CO_2 surface fluxes existing in this region (see Fig. 4a).

The integral of CO_2 convective fluxes over the top of volume V gives the second term of the right-hand side of eq. (2). Its monthly variation is plotted as dotted line in Fig. 3. As compared to the other terms of eq. (2), the convective fluxes are quite small. This is due to the choice of h. Indeed, the higher the top of volume V, the lower the magnitude of convective fluxes. This is illustrated in Fig. 6, which shows the variation of CO_2 convective flux at three different altitudes h at 700 m, 5 km and 8 km. If the maximal altitude of the flights were 5 km instead of 8 km, the convective fluxes would be three times higher. Therefore, CO_2 vertical profiles should be measured up to the highest altitude possible.

However, whatever the maximal altitude of the flights, a direct quantification of convective transport over North America is required. Aircraft campaigns measuring CO_2 vertical profiles during summer, such as the INTEX-NA performed by NASA in July–August 2004, may bring some answers to these questions

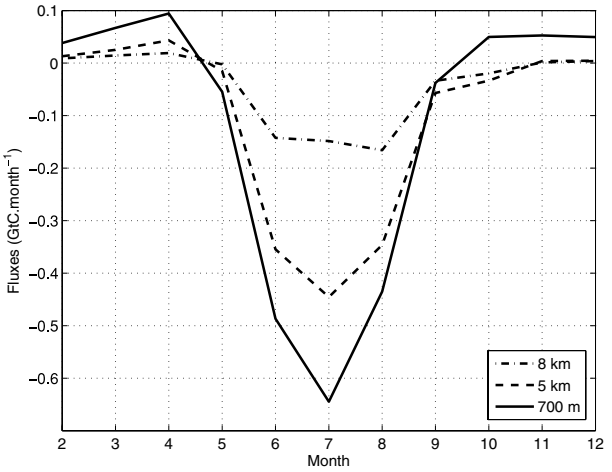

Fig. 6. Monthly variation of convective fluxes simulated by MOZART-2 at an altitude of 700 m (full line), 5 km (dashed line) and 8 km (dash–dotted line).

(S. Vay, personal communication, 2005). More particularly, it must be noted that convective fluxes simulated by MOZART-2 do not take into account deep convection induced by fires. This kind of convection, entraining a large amount of carbon into the upper-troposphere (Fromm et al., 2000), may be encountered in the North American boreal forests affected by large

fires and will need to be taken into account to avoid underestimating the loss of carbon inside the control volume due to this phenomenon.

3.5. Variation of carbon inside the volume

The annual standard deviation of the variation of carbon inside volume V is plotted on Fig. 4d. CO_2 is mainly variable in the northern part of the volume, along the East coast and the northern part of the West coast. This variability follows the location of the surface fluxes and the inflow and outflow pathways of CO_2 inside North America. Fig. 4d thus aggregates all the variations presented in the preceding sections. Summing CO_2 variations in the whole volume on a monthly basis gives the full line plotted in Fig. 3. The huge uptake of carbon in summer, as opposed to the slight emission of CO_2 the rest of the year, can be clearly seen.

4. Data interpolation

The discussion in Section 3 is based on knowing the CO_2 vertical profiles at every gridcell. In reality, CO_2 will only be measured at a given set of stations unevenly distributed over the continent. Therefore, to compute each term of eq. (2), the CO_2 profiles must first be interpolated over the whole volume V. This is achieved here through a geostatistical interpolation technique called Kriging. This method is chosen because it takes into account the observed spatial correlation structure and allows an estimation of the interpolation error.

4.1. Ordinary Kriging

Carbon dioxide spatial distribution varies more or less continuously and may thus be regarded as a random variable distributed in space, a so-called regionalized variable (Matheron, 1965). It is then possible to use a geostatistical approach, like Ordinary Kriging (OK), to interpolate CO_2 on a regular grid. This approach requires the modelling of CO_2 spatial covariance.

Define $Z(r)$ as the spatial random distribution of CO_2 we want to interpolate at location r. The OK model of Z is assumed to be of the form

$$Z(r) = \mu + \varepsilon(r), \tag{4}$$

where μ is the local mean of Z in the neighborhood of r and $\varepsilon(r)$ is a random term with an expectation of zero and a variance such that, for two sampled locations separated by a distance d,

$$\mathrm{Var}[\varepsilon(r) - \varepsilon(r+d)] = 2\gamma(d), \tag{5}$$

where Var denotes the variance and $\gamma(d)$ is called the semivariance between the two locations. If μ is constant locally, then eq. (5) is equivalent to

$$\gamma(d) = \frac{1}{2}\mathrm{Var}[Z(r) - Z(r+d)] = \frac{1}{2}E[Z(r) - Z(r+d)], \tag{6}$$

which defines the variogram γ of Z. The variogram represents the variance between CO_2 measurements made at different locations, as a function of the distance between the locations. It may be seen as an unbiased description of the scale and pattern of Z spatial variations.

Given N measurements $Z(r_i) \quad i = 1, \ldots, N$ of Z at known locations r_i, we want to obtain an estimate $\hat{Z}(r_0)$ of the field at an unsampled location r_0. The OK estimator is obtained when three conditions are reached: (1) $\hat{Z}$ is linear in the $Z(r_i)$, (2) $\hat{Z}$ is unbiased, and (3) $\hat{Z}$ minimizes the mean-square prediction error $E[Z(r_0) - \hat{Z}(r_0)]^2$. This yields the three following equations:

$$\hat{Z}(r_0) = \sum_{i=1}^{N} \lambda_i Z(r_i) \tag{7}$$

$$\sum_{i=1}^{N} \lambda_i = 1 \tag{8}$$

$$\gamma(d_{0j}) = \sum_{i=1}^{N} \lambda_i \gamma(d_{ij}) - \beta_j \quad \text{for } j = 1, \ldots, N, \tag{9}$$

where $d_{ij} = \|r_i - r_j\|$ is the distance between locations i and j and β is a regularization term, which may be seen as a term controlling the smoothness of the solution.

Assuming that the variogram γ is known, solving eqs. (8) and (9) gives access to the interpolation weights λ_i that can then be used to interpolate Z according to eq. (7). A complete description of the interpolation procedure may be found in Marcotte (1991).

Interpolating CO_2 thus requires the determination of its variogram. To take into account any change in spatial structures that might be occurring during the year, variograms are determined on a monthly basis through the use of CO_2 simulations performed at every gridcell. For instance, the experimental

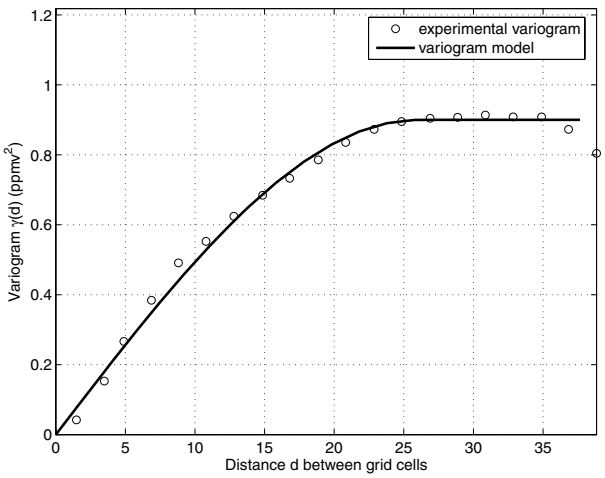

Fig. 7. Experimental variogram (dots) and variogram model (line) obtained from CO_2 simulations for the month of September in the direction of the major axis of elliptic spatial correlation.

variogram obtained for the month of September is shown as open circles in Fig. 7. From these points, a model variogram, shown as full line on Fig. 7, is derived. Given the experimental variogram, we have chosen a classical spherical variogram model defined as

$$\gamma(d) = \begin{cases} C_0 + C\left[\dfrac{3d}{2a} - \dfrac{1}{2}\left(\dfrac{d}{a}\right)^2\right] & \text{if} \quad 0 < d < a \\ C_0 + C \quad \text{if} \quad d \geq a \end{cases}, \qquad (10)$$

where C_0 is called the nugget effect and represents variations at a smaller scale than any of the measured pairwise distances, C is the sill (variance after distance a) and a is the range (distance from which two observations are not linearly linked anymore and thus have a covariance of zero).

As the variations of CO_2 over North America are mostly influenced by the winds, the spatial correlation of CO_2 is not expected to be the same in every direction. To include this anisotropy, the spatial correlation is assumed to have an elliptic structure. A variogram must then be computed for both the major and minor axis of the ellipse. The directions of the axis are determined for each month, by finding the directions with highest and lowest range a. The major axis usually follows the favoured direction of the winds. For instance, in winter, the winds are mainly oriented toward south-east; the major axis of the elliptic spatial correlation is found to be at 35° from the west-east direction.

Due to the use of simulations, the variogram model, plotted in Fig. 7, tends to zero with d, leading to a $C_0 = 0$. In reality, inside one gridcell, CO_2 is expected to be variable and the correlation between different points inside the same gridcell must be taken into account. This is done by setting C_0 to the variance expected inside a grid box. To compute C_0, a method analogue to the one developed by Lin et al. (2004) may be used: from analyses of aircraft observations made over North America during the CO_2 Budget and Rectification Airborne (COBRA) missions in August 2000 and June 2003, Lin et al. (2004) have found a spatial variability of 1–2 ppmv in summer for grid resolutions analogous to the one used in our study. The variability then decreases with the altitude. More campaigns planned in the framework of NACP should improve our knowledge of this variability.

4.2. Application to the NACP network

The Kriging method designed in the previous section is now applied to the 19 NACP sites detailed in Table 1. From the CO_2 simulations obtained at these locations, interpolated CO_2 vertical profiles are computed for every gridcell. The interpolated CO_2 field is then compared to the 'true' value, known from the simulations. Figs. 8a and b show the monthly error obtained for the representative months of January and July. To display every level at once, the error is computed for the column average of CO_2 mixing ratio defined as

$$\bar{\chi}_{CO_2} = \frac{\int_{P_{surf}}^{P_h} \chi \, dP}{\int_{P_{surf}}^{P_h} dP}, \qquad (11)$$

where χ is CO_2 mixing ratio, P is the pressure, P_{surf} the pressure at the surface and P_h the pressure at altitude h.

In winter (Fig. 8a), the interpolation error is low, reflecting the low variability of CO_2 due to the absence of vegetation. In summer (Fig. 8b), the error is higher, due to the exchanges of CO_2 between air and land, and varies more from one region to the other. As expected, the error obtained in regions well covered by NACP sites, mostly on the East, is lower compared to regions, located mostly in the West, where no site is available. However, it can be seen that some differences exist between north-west and south-west, two regions that are not well covered by stations. This is due to the intensity of surface fluxes found in these regions. As can be seen in Fig. 8c, during July, high air-land fluxes are found in the north-west whereas low or no surface fluxes are observed in the South. Therefore, the variability of CO_2 due to its uptake by vegetation during summer is higher in the North than in the South.

More precisely, large errors may be explained by two factors: the surface fluxes and the wind distribution. To illustrate their influence, let us focus on the large error obtained in July in the north-west, north of Montana. The corresponding interpolation error, surface flux, and wind distribution are plotted in Fig. 8b, c and d. In this region, high variability of surface fluxes induces high variability of atmospheric CO_2. To be captured by the network, this variability needs to be transported by the winds toward nearby stations. But, as may be seen in Fig. 8d, the winds coming out of the region mainly have an eastward component and therefore do not reach the other stations that are located further South. Before reaching more easterly stations, the high surface fluxes found along the wind pathway modify atmospheric CO_2 and the signal we are interested in is lost. Therefore, the network does not get information on the variation of CO_2 in the north-west region. A similar explanation may be given for the error found in eastern Canada (regions of Quebec and New Brunswick). To a lesser extent, large errors are also found in the south-east (near North Carolina) and the south-west (near New Mexico), reflecting the lack of stations in these regions. The importance of measuring CO_2 along the trajectory of the wind is well seen in the region south of the Great Lakes. While high surface fluxes of CO_2 still induce high CO_2 variability, seven stations, almost all located along the wind pathway, succeed in capturing this variation: the interpolation error is low.

The error caused by interpolation induces errors on the estimation of each term of eq. (2) and thus on the surface flux estimation. With the 19-station network, the precision achieved on the flux estimation is 0.39 GtC yr^{-1}. This value includes the error due to the variation of carbon inside the control

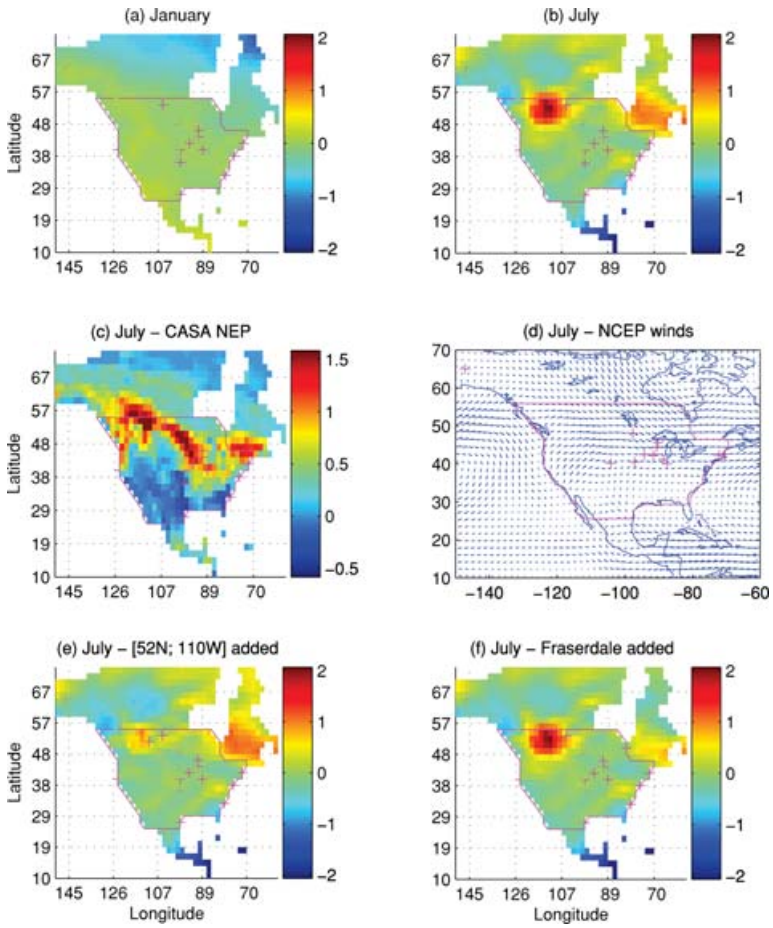

Fig. 8. (a) Interpolation error (ppmv) on CO_2 integrated content for January, (b) same as (a) for July, (c) CASA NEP (GtC month^{-1}) for July, (d) NECP winds for July, (e) interpolation error (ppmv) in July obtained with 19 station network plus a station at 52°N and110°W and (f) same as (e) but with the added station of Fraserdale.

volume (0.25 GtC yr^{-1}), the error on the advective transport (0.12 GtC yr^{-1}) and the lack of a good estimation of convection (0.27 GtC yr^{-1}). It should be noted that this value does not take into account errors that could be due to subgridcell variability missing in the present simulation.

4.3. Improvement of the NACP network

A way to reduce the interpolation error would be to add more stations, in particular in the north-west and north-east. Concerning the north-west, the highest error is found around 110°W, between 50°N and 54°N. Therefore, any station located around 110°W and below 50°N will not improve appreciably the results, since the winds coming from southern regions turn at this latitude and become oriented eastward preventing these air masses from reaching the regions to the North. On the other hand, a station located above 54°N will not bring information on CO_2 variation in the region below this latitude. These two results have been confirmed by simulations (not shown). After performing the interpolation with various networks, composed on the 19 stations detailed in Table 1 plus one station, the best reduction of interpolation error was obtained by adding a station located at 52°N; 110°W. The corresponding interpolation error is shown on Fig. 8e. It is decreased by a factor of 4 in the north-west, and the error on the flux estimation now reaches 0.34 GtC yr^{-1}. However, the interpolation error still remains high above Montana and more stations will certainly be needed to decrease it to the average value obtained over the rest of the continent.

In order to integrate the region of Quebec in volume V, where large flux variations are expected, a station may also be added in the north-east. A good candidate would seem to be the site of Fraserdale in northern Ontario (49°53′N; 81°31′W) where, since 1990, the Meteorological Service of Canada (MSC) measures CO_2 flux by an eddy flux tower and atmospheric CO_2 concentration at the top of a 40 m-tall tower. Measurement of CO_2 vertical profiles at this site would result in a factor of 2 decrease of the interpolation error in the region of Quebec as can be seen on Fig. 8f for which the interpolation has been performed with Fraserdale and the 19 station network. Adding another station located at the same latitude (50°N) and around 70°W could then help decreasing the error in the region of New Brunswick and eastward.

5. Conclusions

Within a synthetic world, a geostatistical interpolation technique has been applied to 'observations' made by a dense network covering North America to infer 3-D CO_2 distribution over the continent. These estimations have then been used, in conjunction with wind distributions, to compute the variation of carbon and advective transports in and out of a control volume above the continent. CO_2 surface fluxes have then been retrieved by the difference between the tendency of carbon inside the volume, and advective and convective transports, with a precision reaching 0.39 GtC yr^{-1}. This value has been obtained with an aircraft profile height of 8 km and has been shown to increase when using profiles reaching a lower altitude, mainly because of the uncertainty due to the amount of carbon transported by convection. Before applying this direct carbon budgeting approach to data obtained at the stations implemented in the framework of the NACP, some questions remain.

First, a better description of subgridcell CO_2 variability and its influence on flux estimation error is needed. The use of spatially highly resolved simulations will give insight on this issue. Such simulations may also help to better resolve the need of stations in some regions. The use of other surface flux simulations, to remove any biases due to the chosen ecosystem model, is also planned.

Second, an accurate estimation of convective fluxes is required to obtain the exchanges between the volume and the upper atmosphere. The use of other tracers (CO, SF_6 and atmospheric potential oxygen) observed during intense short aircraft missions may give some information on convection over North America.

Third, the need of some stations above Montana and near Quebec has been highlighted. Some stations in the south-west and in the south-east may also be added to reinforce the restrained network existing in these regions. Applying the method with CO_2 simulations performed at higher spatial and temporal resolutions will bring more information on regions that potentially need a better coverage.

Additional extensions of the network can also be considered. First, adding some stations in Canada would help constrain the variation of carbon along the border between USA and Canada and would allow an improved description of CO_2 variations in the North American boreal forest. The feasibility of implementing some stations in Canada is studied in the Canadian Carbon Plan directed by the Meteorological Service of Canada (Lin Huang, personal communication, 2005). Another source of high-density observations is the measurements of CO_2 by commercial airliners, which could be used to obtain regular CO_2 vertical profiles in the proximity of airports. Such measurements are, for example, performed in the framework of the Civil Aircraft for the Regular Investigation of the atmosphere Based on an Instrument Container (CARIBIC) project (Brenninkmeijer et al., 1999).

The direct carbon budgeting approach could also be applied to smaller regions, such as the South of the Great Lakes where many stations already exist. Besides, the high-reaching convection affecting this region is lower than in the southern USA.

Finally, the surface fluxes that could be estimated by this approach are the sum of air-land fluxes and anthropogenic emissions. To separate these contributions, observations of other species like CO and SF_6 may possibly be used in concordance with CO_2. Although expensive, the measurement of $^{14}CO_2$ would provide the best way to deal with this problem.

6. Acknowledgements

This research was funded by the Cooperative Institute for Climate Science under award NA17RJ2612 from the National Oceanic and Atmospheric Administration, U.S. Department of Commerce, and by the Carbon Mitigation Initiative, with support provided by the Ford Motor Company. The statements, findings, conclusions and recommendations are those of the authors and do not necessarily reflect the views of the National Oceanic and Atmospheric Administration, or the U.S. Department of Commerce. The authors wish to thank John Dunne for providing the air-sea fluxes used in this study and Lin Huang for fruitful discussions.

References

Adams, D. K. and Comrie, A. C. 1997. The North American monsoon. *Bull. Am. Meteorol. Soc.* **78**, 2197–2213.

Andres, R. J., Marland, G., Fung, I. and Matthews, E. 1996. A one degree by one degree distribution of carbon dioxide emissions from fossil-fuel consumption and cement manufacture, 1950-1990. *Global Biogeochem. Cycles* **10**(3), 419–429.

Blasing, T. J., Broniak, C. T. and Marland, G. 2004. Estimates of monthly carbon dioxide emissions and associated $\delta^{13}C$ values from fossil-fuel consumption in the U.S.A. In Trends: A Compendium of Data on Global Change, Carbon Dioxide Information Analysis Center, Oak Ridge National Laboratory, U.S. Department of Energy, Oak Ridge, TN, U.S.A.

Brenninkmeijer, C. A. M., Crutzen, P. J., Fischer, H., Güsten, H., Hans, W. and co-authors. 1999. CARIBIC - Civil aircraft for global measurement of trace gases and aerosols in the tropopause region. *J. Atmos. Oceanic Technol.* **16**(10), 1373–1383.

Denning, A. S., Fung, I. Y. and Randall, D. 1995. Latitudinal gradient of atmospheric CO_2 due to seasonal exchange with land biota. *Nature* **376**, 240–243, 1995.

Fromm, M., Alfred, J., Hoppel, K., Hornstein, J., Bevilacqua, R. and co-authors. 2000. Observations of boreal forest fire smoke in the stratosphere by POAM III, SAGE II, and lidar in 1998. *Geophys. Res. Lett.* **27**(9), 1407–1410.

Gurney, K. R., Law, R. M., Denning, A. S., Rayner, P. J., Pak, B. and TransCom 3 L2 modelers. 2004. Transcom 3 Inversion Intercomparison: model mean results for the estimation of seasonal carbon sources and sinks. *Global Biogeochem. Cycles* **18**, GB1010.

Horowitz, L. W., Walters, S., Mauzerall, D. L., Emmons, L. K., Rasch, P. J. and co-authors. 2003. A global simulation of tropospheric ozone and related tracers: description and evaluation of MOZART, version 2. *J. Geophys. Res.*, **108**(D24), 4784, doi:10.1029/2002JD002853.

Jacobson, A. R., Mikaloff-Fletcher, S. E., Gruber, N., Sarmiento, J. L., Gloor, M. and TransCom modelers. A joint atmosphere-ocean inversion for surface fluxes of carbon dioxide. II: results. *Global Biogeochem. Cycles*, in press

Lin, J. C., Gerbig, C., Daube, B. C., Wofsy, S. C., Andrews, A. E. and co-authors. 2004. An empirical analysis of the spatial variability of atmospheric CO_2: implications for inverse analyses and space-borne sensors. *Geophys. Res. Lett.* **31**, L23 104, doi:10.1029/2004GL020957.

Marcotte, D. 1991. Cokriging with Matlab. *Comput. Geosci.* **17**(9), 1265–1280.

Matheron, G. 1965. *Les Variables régionalisées et leur estimation*. Masson, Paris, 306 pp.

Randerson, J. T., Thompson, M. V., Conway, T. J., Fung, I. Y. and Field, C. B. 1997. The contribution of terrestrial sources and sinks to trends in the seasonal cycle of atmospheric carbon dioxide. *Global Biogeochem. Cycles* **11**, 535–560.